

## Dyotropic rearrangements of Cp<sub>2</sub>Zr ligand complexes; a theoretical study

G. Narahari Sastry and Eluvathingal D. Jemmis \*

*School of Chemistry, University of Hyderabad, Central University (P.O.), Hyderabad 500 134 (India)*

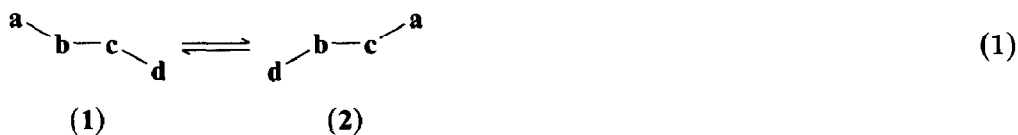
(Received November 13th, 1989)

### Abstract

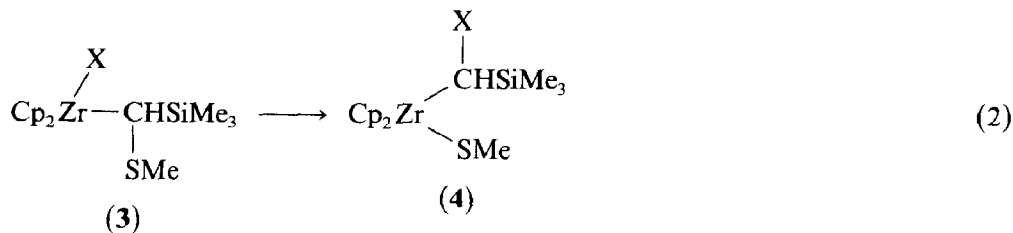
The dyotropic rearrangements in Cp<sub>2</sub>Zr ligand complexes such as Cp<sub>2</sub>Zr(X)(CH<sub>2</sub>SR) (**3**) have been studied by molecular orbital theory. The higher reactivity for the compound with X = Ph in comparison to that with X = Me, Cl, or CH<sub>2</sub>Ph is related to the energy match of MO's of the migrating fragment with those of the remaining fragment along an assumed reaction coordinate. The ease of conversion of Cp<sub>2</sub>Zr(C<sub>4</sub>H<sub>3</sub>O)<sub>2</sub> (**5**) into a zircona-cyclic species **6** can be similarly accounted for. Other substituents that should make the above reactions faster are suggested on the basis of the studies. A general discussion is presented on the migratory aptitudes and the difficulties involved in assigning migratory aptitudes that are independent of the specific reaction.

### Introduction

Isomerisations in which two groups migrate intramolecularly around a bond are called dyotropic rearrangements [1]. Equation 1 represents the prototype of such rearrangements, in which two vicinal groups **a** and **d** migrate around the **b-c** bond. Formation of a three membered intermediate such as  $\overline{\text{a-b-c-d}}$  or  $\overline{\text{a-b-c-d}}$  lowers the activation barrier effectively [2]. Most of the known dyotropic rearrangements take place around C-C bonds [1].

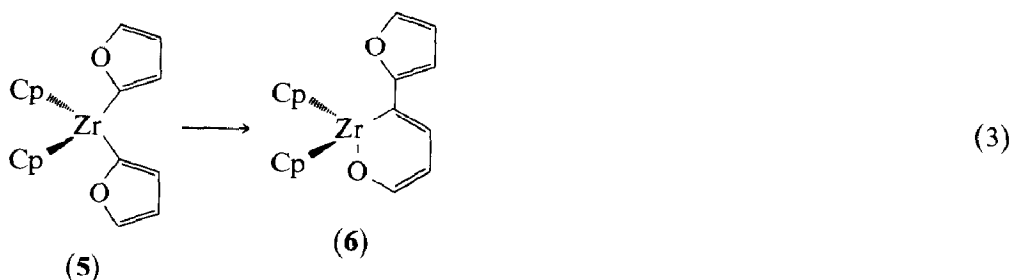


Dyotropic rearrangements are also observed in organotransition metal chemistry. Mintz and coworkers reported a novel dyotropic rearrangement in zirconocenyl thioethers, where  $a = X$ ,  $b = Cp_2Zr$ ,  $c = CH(SiMe_3)$ ,  $d = SCH_3$  (eq. 2) [3]. The reaction proceeds smoothly only for  $X = Ph$ . Kinetic data and labelling and cross-over experiments indicate that it is an intramolecular reaction. A mechanism involving the intramolecular nucleophilic attack of the phenyl group on the methylene carbon has been proposed [3]. The ease of reaction for  $X = Ph$  is attributed to the higher migratory ability of the phenyl groups. When a  $p$ - $C_6H_4OMe$  group is used in place of the Ph group, the reaction is found to take place five times faster [3]. No reaction could be observed for the compounds with  $X = Cl$ , Me or  $CH_2Ph$  under the reaction conditions used.



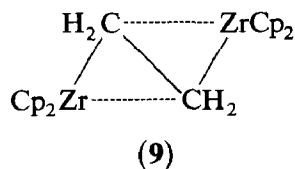
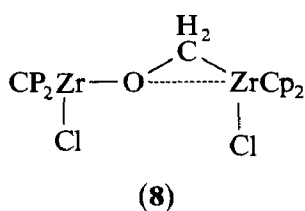
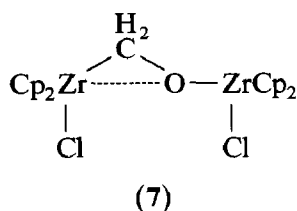
(a:  $X = Ph$ ; b: Me; c:  $CH_2Ph$ ; d: Cl)

Although there is an analogy between  $Cp_2Zr$  and  $CH_2$  [4], more orbitals of various symmetry are available in the frontier region for  $Cp_2Zr$  [5]. The two migrating groups in the eq. 2, a are SMe and Ph. The migration of the SMe group is not strictly similar to that depicted in eq. 1 because the lone pair on sulfur is involved in the initial stages of the reaction. The migration of the phenyl group completes the process. Despite the involvement of the lone pair on sulfur the reaction may be regarded as a dyotropic rearrangement.



A similar reaction was reported recently by Erker and coworkers (eq. 3) [2]. In the above two reactions (eq. 2 and 3) all the changes may be assumed to be taking place in a plane, referred to as the reaction plane. This plane is orthogonal to the plane formed by the two Cp centroids and Zr.

The degenerate rearrangement between **7** and **8** is also an example of a dyotropic rearrangement in organotransition metal chemistry [6]. The two migrating groups are the  $Cp_2Zr$  units. There is already an interaction in the ground state between the migrating group and the terminus, and this considerably reduces the barrier to migration. The structures **7** and **8** are close to that of **9** which has been established by X-ray diffraction studies, and a qualitative molecular orbital picture is available for **9** [7].



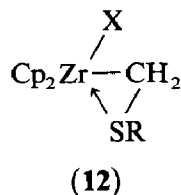
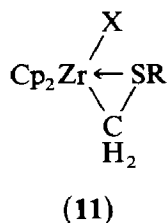
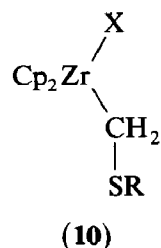
A molecular orbital study of the variations in the barriers to these reactions as a function of the migrating group is presented in this paper. A discussion of migratory aptitudes in general is also given.

Electronic structure studies were carried out by the fragment molecular orbital approach [9] within the extended Hückel approximation [8]. The simplicity of the method, its usefulness in constructing explanations, and the computational economy provided our reasons for using it. The geometric parameters employed in the calculations were taken from the X-ray structures of various related complexes and are shown in the appendix along with the atomic parameters.

## Results and discussion

### *The reaction of $Cp_2Zr(X)CH(SiMe_3)SR$ complexes (Eq. 2)*

The rearrangement indicated by eq. 2 was modelled by use of the complex  $Cp_2Zr(Ph)(CH_2SH)$ . Experimental and theoretical studies on several related complexes had shown that the  $CH_2SR$  group can bind to the Zr centre in three ways,  $\eta^1$ -outside (10),  $\eta^2$ -inside (11),  $\eta^2$ -outside (12) [10]. Of these only the  $\eta^2$ -outside



conformation (12) can serve as the starting point for eq. 2. An NMR study has provided evidence for the existence of the  $\eta^2$ -outside structure for 3 [11], and so this conformation was taken as the starting point for the calculations. In order to understand the electronic structure of the initial complex 3a an interaction diagram was constructed between the fragments  $Cp_2Zr-CH_2$  and  $Ph \cdots SH$ .  $Cp_2Zr-CH_2$  fragment orbitals were obtained from the well-known  $Cp_2Zr$  [5] and  $CH_2$  [12] fragment orbitals (left side of Fig. 1). All the fragment orbitals are labelled in accord with  $C_s$  symmetry. In the  $Cp_2Zr-CH_2$  fragment,  $1a'$  and  $3a'$  are largely  $Cp_2Zr$ -based orbitals and do not change substantially from those for  $Cp_2Zr$  fragment orbitals after interaction with the  $CH_2$  group orbitals. These are the orbitals that interact

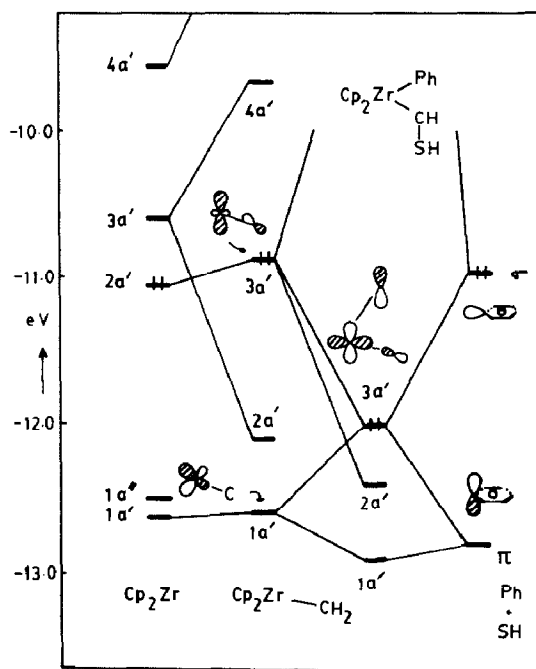


Fig. 1. Construction of the molecular orbitals of  $\text{Cp}_2\text{Zr}(\text{Ph})(\text{CH}_2-\text{SH})$  (**4**) from the fragment orbitals of  $\text{Cp}_2\text{Zr}-\text{CH}_2$  and  $\text{Ph}\dots\text{SH}$  (right). The  $\text{Cp}_2\text{Zr}-\text{CH}_2$  fragment orbitals are in turn obtained from the group orbitals of  $\text{Cp}_2\text{Zr}$  and  $\text{CH}_2$  fragments (left). Only  $\text{Cp}_2\text{Zr}$  orbitals are shown, the  $\text{CH}_2$  orbitals are omitted.

strongly with those of the phenyl group (Fig. 1). Owing to the low symmetry of the resulting molecule (**12**) several multicentre interactions are seen. The HOMO of **12**,  $3a'$ , is part of the four orbital-six electron interaction shown in Fig. 1.  $3a'$  is an antibonding combination of the Zr-C bonding orbital and the Ph  $\pi$ -orbital. The frontier orbitals of the SH group are at lower energies. The sulphur atom of the SH group is bound to C(1) in  $\sigma$  fashion and at the same time the lone pair on sulfur is donated to the Zr centre. A reaction coordinate was constructed for eq. 2 which connects the initial structure **3** and the final structure **4** through equal increments of all the geometric parameters. The Ph group was kept perpendicular to the reaction plane because in the in-plane geometry there are serious steric factors. The positions of C(1) (the methylene carbon), C(2) (the carbon of the migrating group) and S in the reaction plane at different points along the reaction coordinate are plotted in fig. 2, which shows that C(1) has to move markedly more than either C(2) or S during the reaction (since the  $\text{Cp}_2\text{Zr}$  unit is kept fixed during the process). The plot of the sum of one-electron energies for eq. 2, **a** shows a barrier of 16 kcal/mol (Fig. 3) for  $\text{X} = \text{Ph}$ . This is comparable to the experimentally observed value of 20 kcal/mol, for eq. 2, **a**. The product **4a** is calculated to be more stable than the reactant **3a** by about 28 kcal/mol.

The Walsh diagram (Fig. 3a) for this process shows some of the MO's that change maximum along the reaction coordinate.  $C_s$  symmetry is retained during the reaction. HOMO ( $5a'$ ) reproduces the variations of the total energy to some extent. This molecular orbital is initially based on Zr, C(2) and C(1). As the reaction proceeds the antibonding interaction between Zr-C(2) and C(1) in HOMO gets

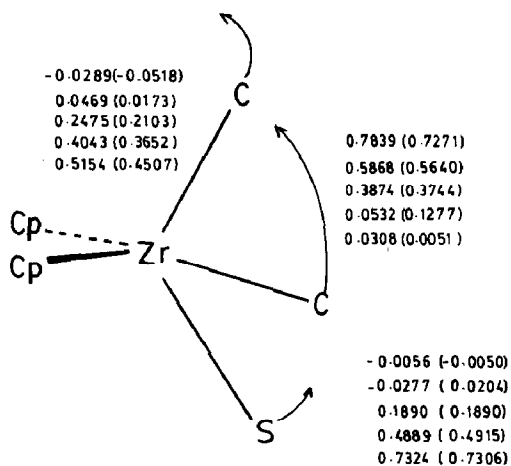


Fig. 2. Positional changes of C(1), C(2) and S along the reaction coordinate as in eq. 2 for  $\text{Cp}_2\text{Zr}(\text{X})(\text{CH}_2\text{-SH})$  going to  $\text{Cp}_2\text{Zr}(\text{CH}_2\text{-X})(\text{SH})$  (eq. 2,a). The corresponding Mulliken overlap population values between Zr-C(2), C(1)-C(2) and C(1)-S along the reaction coordinate are given for X = Ph. The values in the parentheses are those for X = Me.

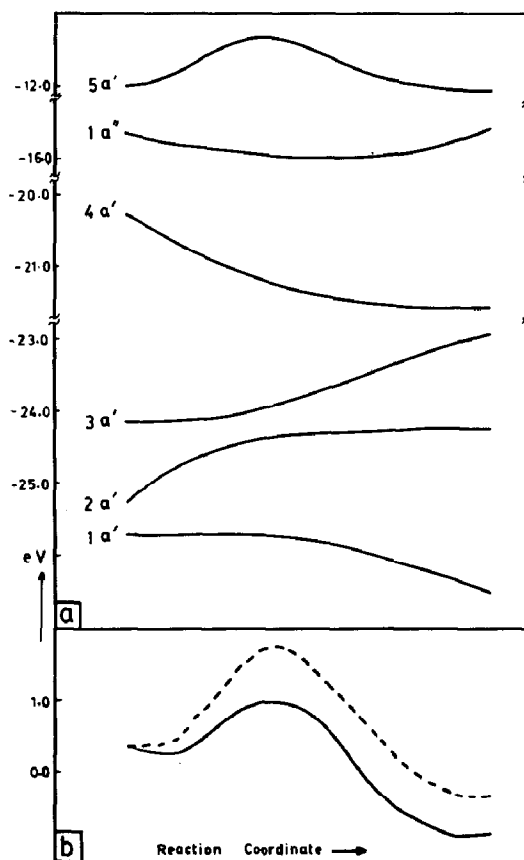
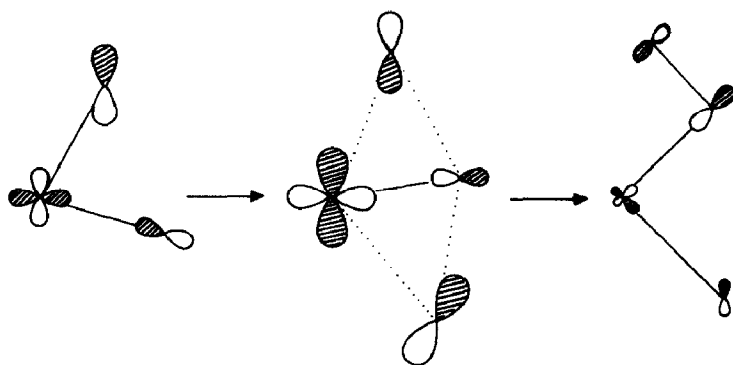


Fig. 3(a) Walsh diagram for  $\text{Cp}_2\text{Zr}(\text{Ph})(\text{CH}_2\text{-SH})$  (3) going to  $\text{Cp}_2\text{Zr}(\text{CH}_2\text{-Ph})(\text{SH})$  (4) (eq. 2,a). Only the orbitals undergoing significant change are shown. (b) The thick line is a plot of the sum of one-electron energies for conversion of 3a into 4a, and the broken line shows the plot of the sum of one-electron energies for the conversion of 3b into 4b.



Scheme 1

stronger and an additional Zr–S antibonding interaction develops until the transition state is reached, as shown in the Scheme 1. But after the energy reaches this maximum it falls as the interaction with S changes from antibonding to bonding with Zr–C(1) bond in the HOMO (Scheme 1). The C–H bonding orbitals of CH<sub>2</sub> (1a'') shows a minimum around the transition state, which lowers the barrier for the process by about 11.5 kcal/mol. At the transition state C(1) is more like an *sp*<sup>2</sup> carbon. One of the reasons for the minimum is the fact that *sp*<sup>2</sup> carbon forms stronger C–H bonds than *sp*<sup>3</sup> carbon. Except for this, the molecular orbitals antisymmetric to the reaction plane are the least affected along the reaction coordinate. Low lying orbitals corresponding to the formation of C–C and Zr–S bonds, and to the cleavage of Zr–C and C–S bonds are the most affected as the reaction proceeds.

The ground state electronic structures of the reactants (**3**) in eq. 2 are not very different for X = Ph and Me, but the presence of a methyl instead of phenyl group prevents the reaction. When the potential energy surface is generated for eq. 2, **b** (i.e. with X = Me) the barrier is about 32 kcal/mol (Fig. 3b), significantly higher than that calculated for eq. 2, **a** (with X = Ph).

The difference between the barriers for the substituents arises mostly from the difference in the stabilisation of the transition states by these substituents. The point of highest energy along the reaction coordinate is regarded as the transition state in this one-electron model. The product **4** is calculated to be more stable than the reactant **3** only by about 16 kcal/mol for X = Me, as against 28 kcal/mol for X = Ph.

To explore further the differences between the compounds with Ph and Me in this reaction (eq. 2), interaction diagrams were constructed at the geometry corresponding to the transition state. In this we consider Cp<sub>2</sub>Zr–CH<sub>2</sub>(SH) as one fragment and X as the other, because there is not much influence of the SH group orbitals in the frontier range. The major interactions of Ph and Me with Cp<sub>2</sub>Zr(CH<sub>2</sub>)SH are shown in Fig. 4. In both the cases the frontier orbital of the X group interacts with the LUMO and an occupied orbital of the metal fragment, leading to a three orbital-four electron interaction. In the ground state the HOMO results from a four orbital–six electron interaction. It has now become a three orbital–four electron interaction because the orientation of the π orbital of Ph is unsuitable for the interaction with the metal fragment orbitals at this transition state

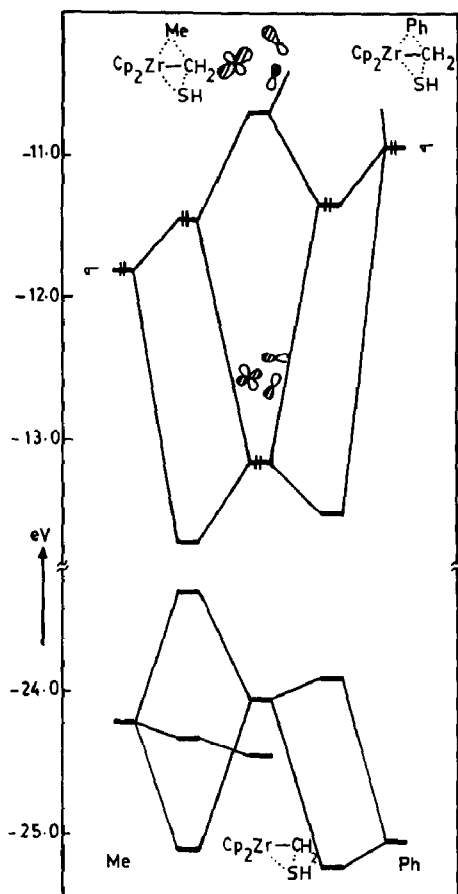


Fig. 4. The orbital interaction diagram of  $\text{Cp}_2\text{Zr}(\text{CH}_2\text{SH})$  fragment with Ph (right) and Me (left) fragments at the transition state.

geometry. For Me or Ph as the migrating group, the middle orbital in the three orbital–four electron interaction HOMO is chiefly responsible for the barrier. The frontier orbital of the Me group lies lower in energy than that of the Ph group. In the three orbital–four electron interaction the Ph  $\sigma$ -bonding orbital interacts more strongly with the LUMO of the metal fragment, whereas the Me  $\sigma$ -bonding orbital interacts more strongly with the occupied orbital of the metal fragment (Fig. 4).

Variations in the low lying orbital energies also effect the barrier [13,14a]. Both the bonding and the antibonding orbitals resulting from the interaction of the low lying orbitals are occupied, so that stronger interactions between these fragment molecular orbitals lead to more destabilisation. There is a strong interaction when  $X = \text{Me}$  in the low lying MO's. Such strong interactions between the two fragments in the transition state results in higher barrier for the reaction. The relative importance of the frontier orbitals compared with lower-lying ones can be investigated by splitting the plot of the sum of one-electron energies into two parts. The first part consists of occupied orbitals of up-to  $-14.975$  eV, which includes the two occupied orbitals in the three orbital–four electron interaction (the frontier region), and the second part includes the remaining low lying orbitals. There is a gap of about 1 eV between these two parts in the Walsh diagram, and there is no crossing

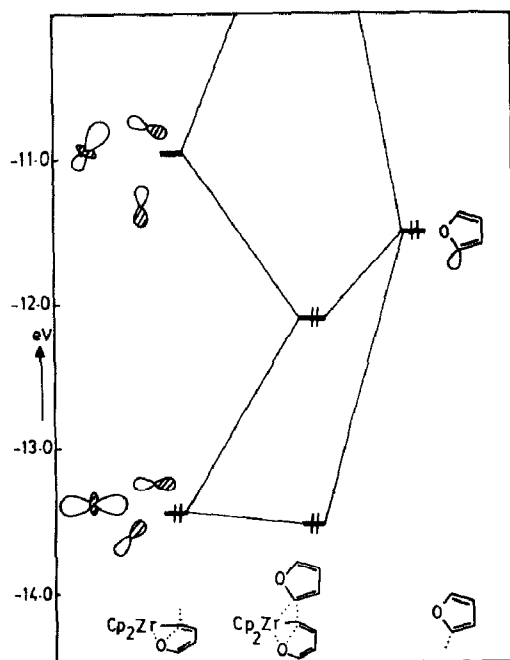


Fig. 5. The orbital interaction diagram between the fragments  $\text{Cp}_2\text{Zr}(\text{C}_4\text{H}_3\text{O})$  and  $\text{C}_4\text{H}_3\text{O}$  at the transition state.

between the levels of the two groups. The first part gives a difference of 7 kcal/mol and the latter 9 kcal/mol for the barrier for the reaction. This shows that the frontier and low lying orbitals are equally responsible for the barrier in this reaction.

Mulliken overlap population values at various points along the reaction coordinate reveal that for eq. 2, **b** the Zr–C(1) and C(1)–C(2) values are less than those for their counterparts for eq. 2, **a**, (Fig. 2). This implies that Ph group could bind simultaneously with the metal and the CH<sub>2</sub> group more strongly than is possible for the Me group. The C–C bond formation starts much earlier in the case of Ph, with considerable retention of the bonding interaction with the metal centre (Fig. 2).

The net charge on the migrating phenyl carbon gradually changes from a high negative value (–0.294) to a positive value (0.088) along the reaction coordinate (eq. 2, **a**). This shows that presence of an electron-donating group on the phenyl ring should favour the reaction. Experimentally the reaction is found to be five times faster for X = *p*-C<sub>6</sub>H<sub>4</sub>OMe than for X = Ph. The net charges on Zr, S, C(1) and C(2) are given in Table 1. As the reaction proceeds the negative charge on C(1) decreases gradually up to the transition state and increases afterwards. This would facilitate the nucleophilic attack of the migrating group on C(1).

The above analysis shows that Ph group has many advantages over Me for the reaction in eq. 2. Since there is not much of a difference between the frontier orbitals of Me and CH<sub>2</sub>Ph we do not find a significant difference between the results for eq. 2, **b** and 2, **c**. Presence of the Cl group also give rise to a high barrier. As expected, in practice the reaction in eq. 2 takes place only with X = Ph. A vinyl group with its π orbital in the reaction plane for X in eq. 2 provides similar frontier orbitals to that of the Ph group. A potential energy surface for eq. 2 when



Table 1

Changes in the net charges on C(1), C(2), S and Zr along the reaction coordinate in eq. 2,a.

Points along the reaction coordinate	ATOM			
	C(1)	C(2)	S	Zr
1	-0.304	-0.294	0.175	0.447
2	-0.116	-0.218	0.032	0.302
3	-0.009	-0.087	-0.316	0.225
4	-0.360	-0.020	-0.531	0.626
5	-0.464	0.061	-0.424	0.745
6	-0.402	0.088	-0.348	0.738

X = CH=CH<sub>2</sub> gives a barrier of about 15 kcal/mol, comparable to that for the Ph substituent. Experimental studies with X = CH=CH<sub>2</sub> should be rewarding.

*The reaction of Cp<sub>2</sub>Zr(C<sub>4</sub>H<sub>3</sub>O)<sub>2</sub> to give the zirconacycle (6) (eq. 3)*

The reaction shown in eq. 3 (formation of the zircona-cycle **6**) shows a close similarity to that in eq. 2. Both involve C–C bond formation, Zr–C bond cleavage, and Zr–O or Zr–S bond formation, followed by C–O or C–S bond cleavage. The reaction coordinate chosen for study of eq. 3 was similar to that for eq. 2. The plot of the sum of one-electron energies shows a barrier of about 10 kcal/mol.

The Walsh diagram shows that the barrier is reproduced to some extent by the HOMO + 2 orbital. An interaction diagram was constructed for this reaction at the transition state for the fragments furanyl and Cp<sub>2</sub>Zr(C<sub>4</sub>H<sub>3</sub>O). In this case the strongest interaction is again a three orbital–four electron one involving the HOMO of the migrating group (furanyl), the LUMO, and an occupied orbital of Cp<sub>2</sub>ZrC<sub>4</sub>H<sub>3</sub>O. HOMO + 2 which reproduced the total energy is the middle orbital in the three orbital interaction. There are also some interactions among low lying orbitals that supplement the effects of the frontier orbitals. In general the controlling factors in eq. 2 and 3 appear to be similar. The potential energy surface is generated for eq. 3 by replacing the migrating furanyl group by Ph or Me. The plot of the sum of one electron energies reveals no barrier when Ph is the migrating group, but migration involves Me a barrier of about 7 kcal/mol. The origin of the low barrier for eq. 3 can be traced to the low lying metal fragment LUMO (–10.95 eV). A low-lying metal fragment LUMO strongly interacts with the HOMO of the migrating group and stabilises the lower two orbitals of the three orbital interaction. In eq. 2 the LUMO of the metal fragment, Cp<sub>2</sub>Zr(CH<sub>2</sub>–SR) is at –10.57 eV. Hence for the same migrating groups there is a large difference between the barriers for these two reactions. If the compounds with Me and Ph were used in the reaction shown in eq. 3, the formation of zircona-cycles should, according to this analysis, be facile.

*On the migratory aptitudes of ligands*

Any migration involves the cleavage of a bond and the formation of another. Barriers for migration reactions are said to be controlled by the migratory abilities of the groups. What are the factors involved in the migration of a group? What are the factors that make the process easier or harder? Is it possible to talk about the

inherent migratory ability of any group independent of the reaction involved? We have attempted to find out the origin of the higher or lower migratory abilities of groups in these reactions. Many theoretical and experimental studies are available on the topic of migrations, in organic as well as organometallic chemistry [14,15]. It has not been possible to assign to groups migratory aptitudes that can be used over a range of reactions. We shall see what difficulties are involved in assigning fixed values to migratory aptitudes of groups independent of the reaction based on the above results.

The three orbital–four electron interaction observed at the transition state is common in the reactions that are studied. For the maximum stabilisation the difference in energy between the  $\sigma$  bonding orbital of the migrating group and the LUMO of the metal fragment should be at a minimum. The extension in space of the  $\sigma$  bonding orbital of the migrating group is also important. It should be so oriented that there is optimum overlap with the LUMO of the metal fragment.

In addition to this there can be other interactions in the lower lying orbitals; these are two orbital–four electron interactions, which lead to destabilisation. Sometimes these will be dominant as in eq. 2, a. Though the HOMO of the furanyl group lies at a higher energy than that of the Me group, a slightly higher barrier is observed for eq. 3 when the substituent is furanyl than when it is Me. This is due to the interactions of low lying orbitals, as can be seen from an interaction diagram for  $X = \text{Me}$  and  $\text{Cp}_2\text{Zr}(\text{C}_4\text{H}_3\text{O})$  at the transition state. This analysis indicates that in organometallic migrations it is not possible to talk in terms of inherent migratory abilities of various groups. Migratory aptitude depends on the total molecule of which the migrating group is a part. What is true of the organometallic compounds must also be applicable to the organic compounds, although the details of the interactions between the migrating group and the organic moiety will differ. This is reflected in differences between the pattern of migratory aptitudes of a set of groups in different reactions. In addition to the electronic effects, the medium used for the reaction should also affect the relative ease of migrations. It is not surprising therefore that parameters defining relative migratory tendencies for various groups applicable to large sets of reactions are not available [15].

## Conclusions

The fact that rearrangement of  $\text{Cp}_2\text{Zr}(\text{X})(\text{CH}_2\text{-SR})$  to give  $\text{Cp}_2\text{Zr}(\text{CH}_2\text{-X})\text{SR}$  takes place for  $X = \text{Ph}$  but not for  $X = \text{Me}$ ,  $\text{CH}_2\text{Ph}$  or  $\text{Cl}$  is attributed to the higher migratory aptitudes of the phenyl groups. Molecular orbital studies by the extended Hückel method has confirmed the view that migratory aptitudes cannot be independent of the reaction. The same set of groups must have different relative migratory aptitudes in different reactions. Only the  $\sigma$  orbital of the migrating group and not the  $\pi$  orbital seems to play a major role in these rearrangements.

The  $\text{Cp}_2\text{Zr}$  fragment in these complexes can be treated as the smallest template on which various transformations can occur. The two Cp units should be above and below the reaction plane (the plane containing the fragment orbitals) and orthogonal to the plane formed by Zr and the centroids of the Cp rings). The large number of frontier orbitals of differing symmetry and extension in space in the reaction plane help to maintain substantial bonding character throughout the reaction coordinate, as can be seen from the Mulliken overlap population values. Hence we

feel that  $\text{Cp}_2\text{Zr}$  fragment may be treated as a mononuclear system closest to that of a template.

### Acknowledgements

The Council of Scientific and Industrial Research, New Delhi is thanked for financial assistance.

### Appendix

The parameters for Extended Huckel calculations for C, H, O and Zr are taken from the previous studies [8,10b].

#### *Geometric parameters used*

Zr–C 2.28, Zr–C(Cp) 2.50, Zr–S 2.48, C(Cp)–C(Cp) 1.40, C–H 1.09, Zr–O 2.16, C–C 1.54, S–H 1.34 Å. Cp–Zr–Cp 126, C(1)–S–H 105°. In **3**, C(1)–Zr–C(2) 75, Zr–C(1)–S 80° and in **4** C(1)–Zr–S 90°. The reaction coordinate is obtained by varying in equal increments all the geometric parameters that change along the reaction coordinate. The variations of the positions of the atoms are shown in Fig. 2 for the eq. 2,a.

### References

- 1 (a) M.T. Reetz, *Adv. Organomet. Chem.*, 16 (1977) 33; (b) M.T. Reetz, *Angew. Chem. Int. Ed. Engl.*, 11 (1972) 129, 131.
- 2 G. Erker, *J. Chem. Soc., Chem. Commun.*, (1989) 345.
- 3 (a) E.A. Mintz, A.S. Ward and D.S. Tice, *Organometallics*, 4 (1985) 1308; (b) A.S. Ward, E.A. Mintz and M.P. Kramer, *ibid.*, 7 (1988) 8.
- 4 (a) H.H. Britzinger and L.S. Bartell, *J. Am. Chem. Soc.*, 92 (1970) 1105; (b) H.H. Britzinger and J.E. Bercaw, *ibid.*, 92 (1970) 6182.
- 5 J.W. Lauher and R. Hoffmann, *J. Am. Chem. Soc.*, 98 (1976) 1729.
- 6 (a) K.I. Gell, G.M. Williams and J. Schwartz, *J. Chem. Soc., Chem. Commun.*, (1980) 550; (b) G. Erker and K. Kropp, *Chem. Ber.*, 115 (1982) 2437.
- 7 (a) W. Kaminsky, J. Kopf, H. Sinn and H.-J. Vollmer, *Angew. Chem.*, 88 (1976) 688; *Angew. Chem. Int. Ed. Engl.*, 15 (1976) 629; (b) A.J. Kos, E.D. Jemmis, P.v.R. Schleyer, R. Gleiter, U. Fischbach and J.A. Pople, *J. Am. Chem. Soc.*, 103 (1981) 4996.
- 8 (a) R. Hoffmann, *J. Chem. Phys.*, 39 (1963) 1397; (b) R. Hoffmann and W.N. Lipscomb, *ibid.*, 36 (1962) 3179; 36 (1962) 3489.
- 9 (a) H. Fujimoto and R. Hoffmann, *J. Phys. Chem.*, 78 (1974) 1169; (b) R. Hoffmann, T.R. Swenson and C.-C. Wan, *J. Am. Chem. Soc.*, 95 (1973) 7644.
- 10 (a) P. Hofmann, P. Stauffert and N.E. Schore, *Chem. Ber.*, 115 (1982) 2153; (b) K. Tatsumi, A. Nakamura, P. Hofmann, P. Stauffert and R. Hoffmann, *J. Am. Chem. Soc.*, 107 (1985) 4440.
- 11 A.S. Ward, E.A. Mintz and M.R. Ayers, *Organometallics*, 5 (1986) 1585.
- 12 W.L. Jorgensen and L. Salem, *The Organic Chemist's Book of Orbitals*, Academic Press, New York, 1973.
- 13 The determinative role played by two centred four electron interactions seen in S. Shaik, R. Hoffmann, C.R. Fisel and R.H. Summerville, *J. Am. Chem. Soc.*, 102 (1980) 4555, also see ref. 14a.
- 14 (a) H. Berke and R. Hoffmann, *J. Am. Chem. Soc.*, 100 (1978) 7224, and refs. cited therein; (b) F.U. Axe and D.S. Marynick, *ibid.*, 110 (1988) 3728 and refs. cited therein; (c) C. Zheng, Y. Apeloig and R. Hoffmann, *ibid.*, 110 (1988) 749.
- 15 J. March, *Advanced Organic Chemistry*, 3rd ed., Mc Graw-Hill, New York, 1985, p. 949–951, and refs. cited therein.